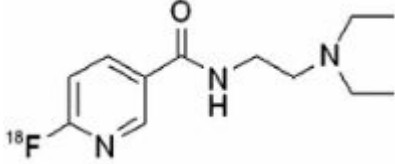


^{18}F -6-Fluoro-N-[2-(diethylamino)ethyl]pyridine-3-carboxamide

^{18}F -MEL050

Liang Shan, PhD¹

Created: August 5, 2011; Updated: September 28, 2011.

Chemical name:	^{18}F -6-Fluoro-N-[2-(diethylamino)ethyl]pyridine-3-carboxamide	
Abbreviated name:	^{18}F -MEL050	
Synonym:		
Agent Category:	Compounds	
Target:	Melanin	
Target Category:	Others	
Method of detection:	Positron emission tomography (PET)	
Source of signal / contrast:	^{18}F	
Activation:	No	
Studies:	<ul style="list-style-type: none"><i>In vitro</i>Rodents	

Chemical structure of ^{18}F -MEL050 (1, 2).

Background

[PubMed]

The probe ^{18}F -6-fluoro-N-[2-(diethylamino)ethyl]pyridine-3-carboxamide, abbreviated as ^{18}F -MEL050, was synthesized by Denoyer et al. for use with melanin-targeted positron emission tomography (PET) of melanoma and its metastasis (1, 2).

¹ National Center for Biotechnology Information, NLM, NIH; Email: micad@ncbi.nlm.nih.gov.

✉ Corresponding author.

NLM Citation: Shan L. ^{18}F -6-Fluoro-N-[2-(diethylamino)ethyl]pyridine-3-carboxamide. 2011 Aug 5 [Updated 2011 Sep 28]. In: Molecular Imaging and Contrast Agent Database (MICAD) [Internet]. Bethesda (MD): National Center for Biotechnology Information (US); 2004-2013.

Melanoma is a highly malignant tumor that originates in melanocytes. The patient's outcome is highly dependent on the early detection of metastasis and on the accuracy of staging. Currently, PET with 2-deoxy-2-[^{18}F]fluoro-D-glucose ([^{18}F]FDG) is routinely used for the staging of melanoma, especially for patients with visceral, deep soft tissue, and lymph node metastases (3). However, [^{18}F]FDG PET suffers from poor sensitivity for the assessment of early stage and small melanomas because of its dependence on glucose metabolism of tumor cells. Lack of specificity of [^{18}F]FDG also makes it difficult to discriminate lymph node metastasis and inflammatory lymphadenopathy (1, 2). In recent years, several other radiolabeled imaging probes have been evaluated for melanoma imaging by targeting melanoma-associated antigens, α -melanocyte-stimulating hormones, and melanin. Of these probes, benzamide (BZ) derivatives are one group of the most promising radiotracers for both diagnosis and therapeutic applications (4, 5).

BZ derivatives represent a versatile class of aromatic compounds that exhibit high and specific binding with melanin in melanoma cells and melanocytes (6, 7). Clinical trials with the agents of [^{123}I]BZA and [^{123}I]BZA2 have demonstrated the high sensitivity and selectivity of these agents in the detection of melanoma and its metastasis (8-10). Because of the promising results, a large series of BZ derivatives are currently under investigation in animal models of melanoma. In general, these agents exhibit comparable *in vitro* properties, but they present different kinetic profiles *in vivo*. Most BZ derivatives exhibit significant liver retention and a predominant clearance *via* the hepatobiliary system, which potentially limits detection of abdominal lesions (1, 11).

Denoyer et al. synthesized a series of fluoronicotinamide compounds (1, 2, 11). The enhanced hydrophilicity of the pyridine nitrogen allows for rapid clearance of the compounds *via* renal excretion. The nicotinamide structure is amenable to direct nucleophilic substitution *via* a rapid, one-step synthesis that provides a means for high-yield incorporation of the ^{18}F into these molecules. These ^{18}F -labeled compounds, including ^{18}F -MEL050, exhibited high radiochemical stability, excellent tumor uptake, and favorable pharmacokinetic properties with excretion predominantly *via* the renal route (1, 2, 11). These positive characteristics suggest that these agents are potentially valuable as PET agents for early detection of melanoma and its metastasis.

This chapter summarizes the data obtained with ^{18}F -MEL050 (1, 2).

Related Resource Links:

[Melanin-targeted imaging agents in MICAD](#)

[Benzamide derivatives in PubChem](#)

[Benzamide derivatives in clinical trials in ClinicalTrials.gov](#)

Synthesis

[\[PubMed\]](#)

The agent of ¹⁸F-MEL050 was prepared from 6-chloro-*N*-[2-(diethylamino)ethyl]pyridine-3-carboxamide precursor with a one-step radiosynthesis by using no-carrier-added ¹⁸F-KF-Krytpofix 222 (dimethylformamide, 150°C, 5 min), followed by purification with high-performance liquid chromatography (1, 2, 11). The synthesis time was 60 min, with an end-of-synthesis yield of 35%–40%, a radiochemical purity of >99%, and a specific activity of 150–220 GBq/μmol (4.05–5.95 Ci)/μmol. The final product was stable (>98%) in saline over 3 h.

In Vitro Studies: Testing in Cells and Tissues

[PubMed]

No data are currently available.

Animal Studies

Rodents

[PubMed]

In one paper published by Denoyer et al., the investigators tested the feasibility of PET imaging with ¹⁸F-MEL050 in the detection of melanoma and its lung metastasis in animal models (1). The organ uptake was calculated from the PET images and expressed as percent of injected dose per gram of tissue (% ID/g) (assuming a density of 1 g/cm³). The background region was chosen to represent the mediastinal blood pool, excluding regions of tracer accumulation such as the spleen.

In a subcutaneous B16-F0 allograft model in C57BL/6 mice ($n = 6$), PET imaging was performed after tail vein injection of 29.6 MBq (0.8 mCi) ¹⁸F-MEL050 (1). Images revealed excellent tumor delineation as early as 1 h after injection. The tumor uptake was relatively constant over the 3-h scanning period (9.6 ± 0.5 , 9.3 ± 0.7 , and 9.0 ± 0.6 at 1, 2, and 3 h, respectively). The tumor/background ratio increased from 19.3 at 1 h to 50.9 at 2 h, reaching 54.3 at 3 h after injection. Accumulation in the bladder, eyes, spleen, and thyroid was visualized, but accumulation in the bone and other organs was not. The radioactivity levels (% ID/g) in the eyes and spleen were also relatively constant, being 2.9 ± 0.2 , 2.2 ± 0.1 , and 1.7 ± 0.04 in eyes and 3.7 ± 0.4 , 2.9 ± 0.4 , and 2.6 ± 0.4 in spleen at 1, 2, and 3 h, respectively, after injection. In contrast, the thyroid uptake dropped by >70% between 1 h and 3 h (2.2 ± 0.2 versus 0.6 ± 0.04), rendering the thyroid signal barely detectable at 3 h. Blocking the thyroid by giving mice drinking water supplemented with Lugol's solution for 3 days before ¹⁸F-MEL050 PET failed to inhibit thyroid uptake (data not shown). The high level of radioactivity in the bladder indicated that ¹⁸F-MEL050 was rapidly and primarily excreted through the urinary system.

In pigmented and unpigmented melanoma models, PET imaging was performed at 1 h after injection of 22.2 MBq (0.6 mCi) ¹⁸F-MEL050 to test the specificity of ¹⁸F-MEL050 (1). Accumulation of the ¹⁸F-MEL050 was observed in the pigmented B16-F0 tumors in

C57BL/6 mice, whereas no significant signal was detected in A375 amelanotic melanoma xenografts in BALB/c nude mice. High-resolution autoradiography of *ex vivo* tumor sections showed that ^{18}F -MEL050 was specifically retained in melanin-containing cells across the entire section of tumor, whereas there was virtually no signal in the unpigmented tumor section. Strong concordance was observed between the ^{18}F -MEL050 autoradiographic signals and the brown melanin-pigmented metastasis.

In a B16-BL6 lung metastasis model in BALB/c nude mice ($n = 4$), mice were imaged on a clinical PET/CT scanner at 1 h after injection of 18–20 MBq (0.49–0.54 mCi) ^{18}F -MEL050 (1). Presence of melanoma lesions in the lungs was clearly visualized, and the ^{18}F -MEL050 signal in the PET/CT images corresponded to the degree of melanoma invasion of the lung tissue under necroscopy.

For comparison, B16-F0 tumor-bearing mice were scanned with [^{18}F]FDG (17.7 MBq (0.48 mCi)) and ^{18}F -MEL050 (20.13 MBq (0.54 mCi)), respectively, at 2 h after tracer injection ($n = 6$ mice) (1). The tumor/background ratio was ~9-fold higher for ^{18}F -MEL050 (50.9 ± 6.9) than for [^{18}F]FDG (5.8 ± 0.5). ^{18}F -MEL050 yielded a much clearer delineation and superior image of melanoma lesions than [^{18}F]FDG.

In another paper published by Denoyer et al., the investigators tested the feasibility of using ^{18}F -MEL050 in the detection of B16-BL6 metastasis in the left popliteal lymph nodes (PLNs) in C57BL/6 mice ($n = 49$) (2). PET was performed at 2 h after systemic (20–25 MBq (0.54–0.68 mCi)) (systemic group, $n = 24$ mice) or subcutaneous perilesional injection (1–1.5 MBq (0.03–0.04 mCi)) (local group, $n = 25$ mice) of ^{18}F -MEL050. Mice were euthanized after imaging for *ex vivo* analysis.

Overall, the radioactive distribution in the mouse body was similar for the two routes of administration, but tracer uptake in the positive PLNs and at the tumor sites was considerably higher in the local group than in the systemic group. ^{18}F -MEL050 accumulation was also observed in normal tissues, including the eyes, spleen, thyroid, kidneys, and bladder, with weaker signal in the local group.

The PET scans on day 5 after tumor implantation showed positive PLNs in three of the 24 mice in the systemic group, with node/background ratios of 4.6, 1.9, and 14.0, respectively. Of the 25 mice in local group, five PLNs were judged as positive on the PET scans, and four of the five positive PLNs had uptake ratios between 47 and 68; the remaining PLN (the smallest node) had a ratio of 16. One mouse in the systemic group appeared to have lung metastasis. In the scan on day 9, three more mice in the systemic group and four mice in the local group showed evidence of lung metastases without node involvement. In the scan on day 14, a signal was observed in the subiliac node of a single mouse from the systemic group. The mean uptake level for positive PLNs was $14.2 \pm 2.9\%$ ID/g in the systemic group and $197.6 \pm 24.4\%$ ID/g in the local group. The mean radioactive level for the negative left PLNs was also higher in the local group (8.5 ± 1.7 , $n = 16$) than in the systemic group (1.7 ± 0.3 , $n = 15$), which may be explained by the fact that more tracers are absorbed into the local lymphatic system and accumulated nonspecifically in the lymph nodes with local injection than with systemic injection. For

contralateral PLNs (right side), the level (% ID/g) was almost the same for the two routes of administration (2 ± 0.6 for systemic and 2.7 ± 0.7 for local) on the basis of five pools, each containing three to five right PLNs. The low radioactivity detected in the negative PLNs in both sides may represent the non-specific retention of the agent.

Lymph node metastasis was also examined with ultrasound, confirmed *ex vivo* under necroscopy, and quantified with *ex vivo* counting and polymerase chain reaction (PCR)-based tumor burden analysis. Ultrasound correctly identified 90% of positive PLNs, with one false-positive. ¹⁸F-MEL050 PET correctly identified 60% of positive PLNs after systemic administration and 100% after local administration, with no false-positive results by either route. PET detection efficiency is ~7-fold higher for local than for systemic administrations. The average node/background ratio for positive PLNs was 6.8 in the systemic group and correlated with the PCR-based tumor burden ($R^2 = 0.9764$). In the local group, the mean uptake ratio was 48, without clear relation to metastatic burden ($R^2 = 0.1635$) (2).

Other Non-Primate Mammals

[PubMed]

No references are currently available.

Non-Human Primates

[PubMed]

No references are currently available.

Human Studies

[PubMed]

No references are currently available.

References

1. Denoyer D., Greguric I., Roselt P., Neels O.C., Aide N., Taylor S.R., Katsifis A., Dorow D.S., Hicks R.J. *High-contrast PET of melanoma using (18)F-MEL050, a selective probe for melanin with predominantly renal clearance.* J Nucl Med. 2010;51(3):441–7. PubMed PMID: 20150254.
2. Denoyer D., Potdevin T., Roselt P., Neels O.C., Kirby L., Greguric I., Katsifis A., Dorow D.S., Hicks R.J. *Improved detection of regional melanoma metastasis using 18F-6-fluoro-N-[2-(diethylamino)ethyl] pyridine-3-carboxamide, a melanin-specific PET probe, by perilesional administration.* J Nucl Med. 2011;52(1):115–22. PubMed PMID: 21149487.
3. Muller S.P. *Malignant melanoma: PET/CT as a staging procedure.* Front Radiat Ther Oncol. 2006;39:159–70. PubMed PMID: 16394679.

4. Oltmanns D., Eisenhut M., Mier W., Haberkorn U. *Benzamides as melanotropic carriers for radioisotopes, metals, cytotoxic agents and as enzyme inhibitors*. *Curr Med Chem*. 2009;16(17):2086–94. PubMed PMID: 19519383.
5. Maisoniaux A., Kuhnast B., Papon J., Boisgard R., Bayle M., Vidal A., Auzeloux P., Rbah L., Bonnet-Duquennoy M., Miot-Noirault E., Galmier M.J., Borel M., Askienazy S., Dolle F., Tavitian B., Madelmont J.C., Moins N., Chezal J.M. *Single photon emission computed tomography/positron emission tomography imaging and targeted radionuclide therapy of melanoma: new multimodal fluorinated and iodinated radiotracers*. *J Med Chem*. 2011;54(8):2745–66. PubMed PMID: 21417462.
6. Eisenhut M., Hull W.E., Mohammed A., Mier W., Lay D., Just W., Gorgas K., Lehmann W.D., Haberkorn U. *Radioiodinated N-(2-diethylaminoethyl)benzamide derivatives with high melanoma uptake: structure-affinity relationships, metabolic fate, and intracellular localization*. *J Med Chem*. 2000;43(21):3913–22. PubMed PMID: 11052796.
7. Chezal J.M., Papon J., Labarre P., Lartigue C., Galmier M.J., Decombat C., Chavignon O., Maublant J., Teulade J.C., Madelmont J.C., Moins N. *Evaluation of radiolabeled (hetero)aromatic analogues of N-(2-diethylaminoethyl)-4-iodobenzamide for imaging and targeted radionuclide therapy of melanoma*. *J Med Chem*. 2008;51(11):3133–44. PubMed PMID: 18481842.
8. Bacin F., Michelot J., Bonafous J., Veyre A., Moreau M.F., Kemeny J.L., Chossat F., Bekhechi D. *Clinical study of [123I] N-(2-diethylaminoethyl)-4-iodobenzamide in the diagnosis of primary and metastatic ocular melanoma*. *Acta Ophthalmol Scand*. 1998;76(1):56–61. PubMed PMID: 9541435.
9. Chehade F., De Labriolle-Vaylet C., Michelot J., Moins N., Moreau M.F., Hindie E., Papon J., Escaig F., Galle P., Veyre A. *Distribution of I-BZA (N-2-diethylaminoethyl-4-iodobenzamide) in grafted melanoma and normal skin: a study by secondary ion mass spectroscopy*. *Cell Mol Biol (Noisy-le-grand)*. 2001;47(3):529–34. PubMed PMID: 11441960.
10. Michelot J.M., Moreau M.F., Veyre A.J., Bonafous J.F., Bacin F.J., Madelmont J.C., Bussiere F., Souteyrand P.A., Mauclair L.P., Chossat F.M. et al. *Phase II scintigraphic clinical trial of malignant melanoma and metastases with iodine-123-N-(2-diethylaminoethyl 4-iodobenzamide)*. *J Nucl Med*. 1993;34(8):1260–6. PubMed PMID: 8326382.
11. Greguric I., Taylor S.R., Denoyer D., Ballantyne P., Berghofer P., Roselt P., Pham T.Q., Mattner F., Bourdier T., Neels O.C., Dorow D.S., Loc'h C., Hicks R.J., Katsifis A. *Discovery of [18F]N-(2-(diethylamino)ethyl)-6-fluoronicotinamide: a melanoma positron emission tomography imaging radiotracer with high tumor to body contrast ratio and rapid renal clearance*. *J Med Chem*. 2009;52(17):5299–302. PubMed PMID: 19691348.